Available online at www.sciencedirect.com
ScienceDirect
Physica C 463–465 (2007) 410–414
PHYSICA C
www.elsevier.com/locate/physc

Evaluation of current distribution in bulk superconductors magnetized by pulsed-fields

K. Yokoyama [a,*], T. Oka [b], H. Fujishiro [c], K. Noto [c]

[a] Ashikaga Institute of Technology, 268-1 Omae-cho, Ashikaga, Tochigi 326-8558, Japan
[b] Niigata University, 8050 Igarashi-2nocho, Niigata, Niigata 950-2181, Japan
[c] Iwate University, 4-3-5 Ueda, Morioka, Iwate 020-8551, Japan

Accepted 16 February 2007
Available online 2 June 2007

Abstract

For theoretical clarification of mechanism of a pulsed-field magnetization (PFM) and development of more efficient PFM method, we carried out a detailed computer simulation in consideration of the difference in the superconducting characteristics between the growth sector boundary (GSB) and the growth sector region (GSR) parts of the material. The superconducting current was defined in each part and the magnetic field induced by the local current was calculated. The entire magnetic field distribution was obtained by adding individual distributions. The experiment with a Sm123 bulk superconductor was performed and it was confirmed that the calculated distribution reproduces the experimental one.

PACS: 74.72.−h; 74.25.Ha

Keywords: RE123 bulk superconductor; Critical current density; Magnetic field distribution; Pulsed-field magnetization; Growth sector boundary/region

1. Introduction

According to the recent improvement in the performance of high-T_c REBaCuO (RE = Y, Sm, Gd, etc.) bulk superconductors, a high trapped field exceeding 17 T has been achieved [1]. A superconducting bulk magnet, in which a bulk superconductor is magnetized and used like a permanent magnet, is attracting much attention as one of the applications of bulk materials, because it can generate stronger magnetic field than that of permanent magnets or iron-cored electromagnets. Thus, various industrial applications such as magnetic separation and magnetron spattering are considered [2–5]. In the magnetization, a pulsed-field magnetization (PFM) method is an important technique for various industrial applications, because a bulk can be magnetized with a simple and relatively cheap apparatus in a short time. However, there is a problem that the strength of trapped field (B_T) is less than a half of that magnetized by a field cooled method (FC) at low temperature below about 50 K. The IMRA (iteratively magnetizing pulsed-field operation with reducing amplitudes) method [6,7], MPSC (multi-pulse technique combined with a stepwise cooling) method [8] and MMPSC (modified MPSC) method [9] are developed recently aiming at improvement of B_T in PFM (B_T^{PFM}) and B_T^{PFM} of over 5 T is achieved with the MMPSC method. These are magnetizing methods in which several pulsed-fields are applied with changing the strength of magnetic fields and cooled down temperature based on the idea of controlling heat generation of the bulk during the magnetization. The heat generation influences a critical current density J_c, and thus, the resulted B_T also changes [10,11]. Moreover, it is known that there is a difference in J_c characteristics between a growth sector boundary (GSB) part and a growth sector region (GSR) part in the same material, and the characteristics of the former are more excellent than that of the latter. In the FC magnetization, the difference between two parts hardly influences the

* Corresponding author. Tel.: +81 284 62 0605; fax: +81 284 62 4633.
E-mail address: k-yokoyama@ashitech.ac.jp (K. Yokoyama).

0921-4534/$ - see front matter
doi:10.1016/j.physc.2007.05.027

performance of the trapped field because, in this case, heat generation is mostly caused by the flux flow during the decreasing exciting field which is very slow in FC method, and thus the temperature rise is very small. In the PFM, on the other hand, heat generation originates mainly from flux jump and it is different locally according to the J_c characteristics.

This paper presents a detailed computer simulation taking into the consideration of the difference in the J_c characteristics between GSB and GSR parts for the purpose of theoretical clarification of magnetizing mechanism and development of more efficient magnetizing method. Firstly, a Sm123 bulk superconductor is magnetized by PFM with changing the magnitude of applied peak field from 3.10 to 5.42 T. Temperature and trapped field at the bulk surface are monitored during the magnetization, and the trapped field distribution of 3.5 mm above the surface is scanned after the magnetization. The FC magnetization with varying temperature of the material was also performed. Next, the maximum temperature is obtained from the experimental data of the PFM, and the J_c at that temperature is calculated by using the trapped field-versus-temperature data of the FC assuming that a critical current flows to the entire sample. Here, the current density of GSB and GSR parts is defined, respectively based on the obtained J_c. Then, changing each current density, the magnetic field distribution is simulated and compared with the experimental distribution map. From these procedures, the validity of the simulation is verified from the agreement between experimental and numerical results when the pulsed-field of different magnitude is applied to a bulk superconductor.

2. Experimental

2.1. Experimental detail

Using a melt-processed Sm123 bulk superconductor, a temperature rise and a trapped field distribution in the FC and the PFM are measured. The bulk material is a highly *c*-axis oriented crystal and consists of $SmBa_2Cu_3O_y$ (Sm123), Sm_2BaCuO_5 (Sm211) with the molar ratio of 1.0:0.3, 0.5 wt.% Pt powder and 1.5 wt.% Ag_2O addition (Dowa Mining Co., Ltd.). The sample size is 45 mm in diameter and 18 mm in thickness, and it is impregnated by epoxy resin reinforced by glass fiber. The epoxy resin on the upper and lower sides of the bulk was removed in order to establish the thermal contact to the thermocouples and to measure the precise temperature and to reduce a thermal contact resistance to the cold head. The bulk is set on a copper base connected to a cold head of GM refrigerator (AISIN SEIKI CO., LTD, GR301). Five Teflon-coated chromel-constantan thermocouples (T1–T5) of 76 μm in diameter are adhered on the surface of bulk superconductor using the GE7031 varnish. T1 is put on the center of the bulk. T2–T3 and T4–T5 are arranged in the radial direction of GSR and GSB, respectively as shown in the insets of Fig. 2. A Hall sensor (F.W. Bell, BHT-921) is set near T1 to monitor a magnetic flux density of trapped field as shown also in the insets. A superinsulation is wound around the bulk superconductor and they are covered with a vacuum vessel.

In the FC magnetization, a static field of 5 T is applied by a 10 T superconducting magnet at the higher temperature than a critical one, T_c, and the bulk is cooled down to a prescribed temperature (40, 50, 60 and 70 K at the cold stage). Then, the magnetic field is reduced to zero with a sweep rate of −5.06 mT/s. The temperature and magnetic field are measured every 8 s. In the PFM, after the bulk is cooled down to 40 K at the cold stage, pulsed-field of 3.10, 3.83, 4.64 and 5.42 T with a rising time of 10 ms is applied by using a copper coil cooled at liquid nitrogen temperature and a pulse generator with a condenser bank of 60 mF. The temperature and magnetic field are monitored about 7 times per second. After each magnetization, the trapped field distribution of parallel direction to the bulk axis is measured by scanning an axial type Hall sensor (F.W. Bell, BHA-921) above the vacuum vessel, in which the gap between the bulk surface and the sensor is 3.5 mm.

2.2. Experimental results

Fig. 1 shows the temperature dependence of trapped field. The horizontal and vertical axes indicate the maximum temperature at T1 and the maximum *z*-direction field measured 3.5 mm above the bulk surface, respectively. The relationship in the FC magnetization is also presented. The temperature increases monotonously with the applied field. On the other hand, the trapped maximum field increases with the applied pulsed-field from $\mu_0 H = 3.10$ to 4.64 T, but, thereafter it decreases along the FC line which indicates the upper limit of trapped field for each temperature.

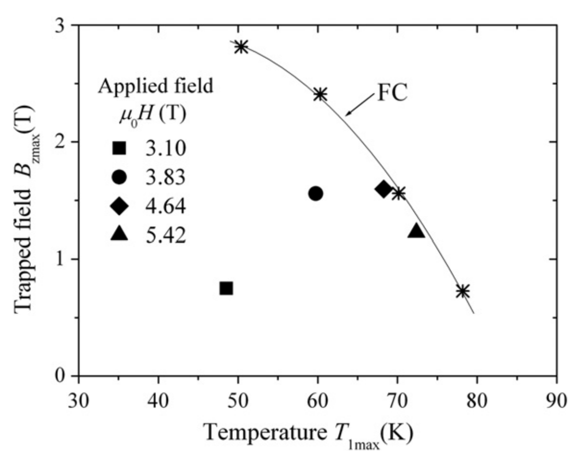

Fig. 1. The temperature dependence of the trapped field for the various applied pulsed-fields. The horizontal and vertical axes indicate the maximum temperature at T1 and the maximum *z*-direction flux density in the horizontal plane 3.5 mm above the bulk surface, respectively. The relationship for the FC magnetization is also presented.

These results suggest that a high applied field causes high temperature rise, and thus, a trapped field is reduced due to the decrease in J_c.

Fig. 2 shows the time response of normalized temperature rise of T1–T5 for pulsed-field of (a) $\mu_0H = 3.83$ T and (b) $\mu_0H = 4.64$ T, respectively. For the case of $\mu_0H = 3.83$ T, the temperature of GSR part (T2, T3) rises faster than that of GSB part (T4, T5) and it means that magnetic flux enters in the bulk through the GSR part. For the case of $\mu_0H = 4.64$ T, on the other hand, the temperature rises up at the same time at all the points and it is considered that magnetic flux enters in the bulk from the whole periphery.

Fig. 3 illustrates the trapped field distribution measured 3.5 mm above the bulk surface for applied pulsed-field of (a) $\mu_0H = 3.83$ T and (b) $\mu_0H = 4.64$ T, respectively. In Fig. 3a, the distribution map draws a diamond shape and one can see that a lot of magnetic flux is trapped in the GSR part. In Fig. 3b, the map is quadrangle and one can see that the trapped flux of GSB part is more than that of GSR. From the results of Figs. 2 and 3, in the case of $\mu_0H = 3.83$ T, an applied field is too small to invade into

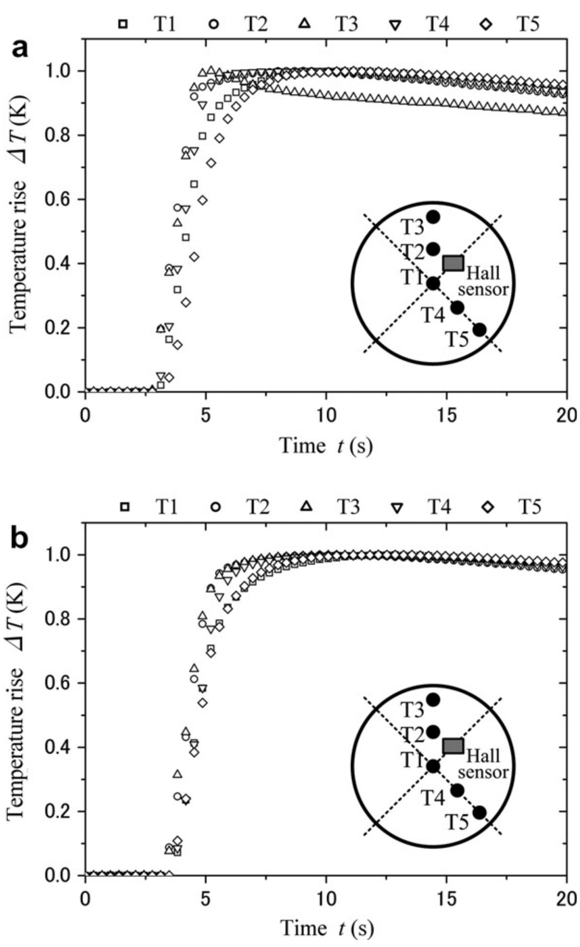

Fig. 2. The time responses of normalized temperature rise at T1–T5 for the applied pulsed-field of (a) $\mu_0H = 3.83$ T and (b) $\mu_0H = 4.64$ T, respectively.

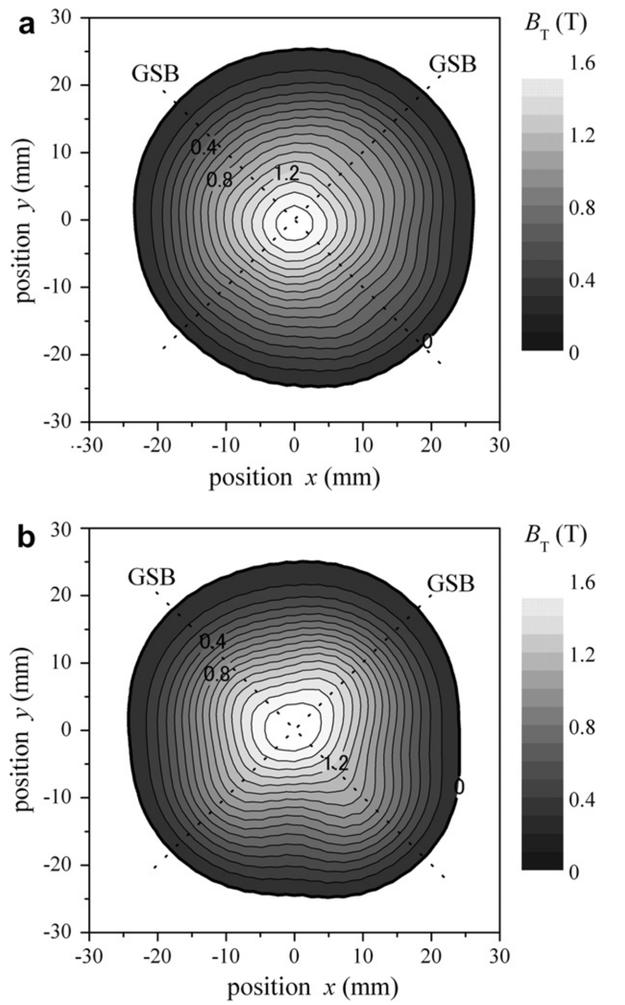

Fig. 3. Trapped field distributions in the horizontal plane 3.5 mm above the bulk surface for the applied pulsed-field of (a) $\mu_0H = 3.83$ T and (b) $\mu_0H = 4.64$ T, respectively (Section 2.2).

the GSB part where J_c is higher. In the case of $\mu_0H = 4.64$ T, on the other hand, magnetic flux can enter into the GSB part, but flux creep occurs because of a decline in J_c caused by large heat generation in GSR part, and then, trapped field decreases.

3. Simulation

In the simulations of magnetization, an axisymmetric model has been usually used. In order to verify the magnetizing mechanism in detail, it is necessary to discuss the GSB and the GSR parts separately because the J_c characteristics are different between each area. This paper attempts to estimate each J_c in two parts by using experimental data and to simulate the magnetic field distribution. In the paper, though the pinning characteristics during the magnetization are not considered, they are evaluated as distribution of J_c after the magnetization.

An analytical procedure is explained in the applied field of 3.83 T. A maximum temperature of $T_{max} = 57.5$ K is obtained from the experimental data. The J_c at 57.5 K can be calculated by using the trapped field-versus-temperature data of the FC magnetization is shown in Fig. 1. Assuming that critical current flows to the whole material, the following expressions for the J_c and the magnetic field density B at an arbitrary position are obtained:

$$\left.\begin{aligned} B &= \mathrm{rot}\,A \\ \frac{1}{\mu_0}\nabla^2 A &= J_c \end{aligned}\right\}, \tag{1}$$

where A and μ_0 are the vector potential and the magnetic permeability of the vacuum, respectively. Now, flux density at the center axis of the bulk 3.5 mm above the surface is $B_T^{3.5\,\mathrm{mm}} = 1.56$ T in Fig. 3a, and therefore, the critical current density is $J_c = 5.18 \times 10^8$ A/m^2 from Eq. (1). Next, the current density in GSB and GSR parts is defined as J^{GSB} and J^{GSR}, respectively, based on the above J_c. The sample is evenly divided into eight regions, each four regions of GSB and GSR. Assuming the current loops in each part, the magnetic field induced by J^{GSB} and J^{GSR} is calculated by use of the Biot–Savart law. The entire magnetic field distribution is obtained by adding individual distributions. After comparing the obtained distribution with the experimental one shown in Fig. 3a, J^{GSB} and J^{GSR} are updated and the magnetic distribution is calculated again. Fig. 4a shows the simulation result when $J^{GSR}/J^{GSB} = 0.3$. The simulation in $\mu_0 H = 4.64$ T is performed as well. The $T_{max} = 65.7$ K and $B_T^{3.5\,\mathrm{mm}} = 1.60$ T from Fig. 3b, and the critical current density is $J_c = 5.89 \times 10^8$ A/m^2. Fig. 4b illustrates the simulation result when $J^{GSR}/J^{GSB} = 1.5$. The numerical results shown in Fig. 4 reproduce the experimental results shown in Fig. 3 well, and thus, the validity of the proposed method is confirmed.

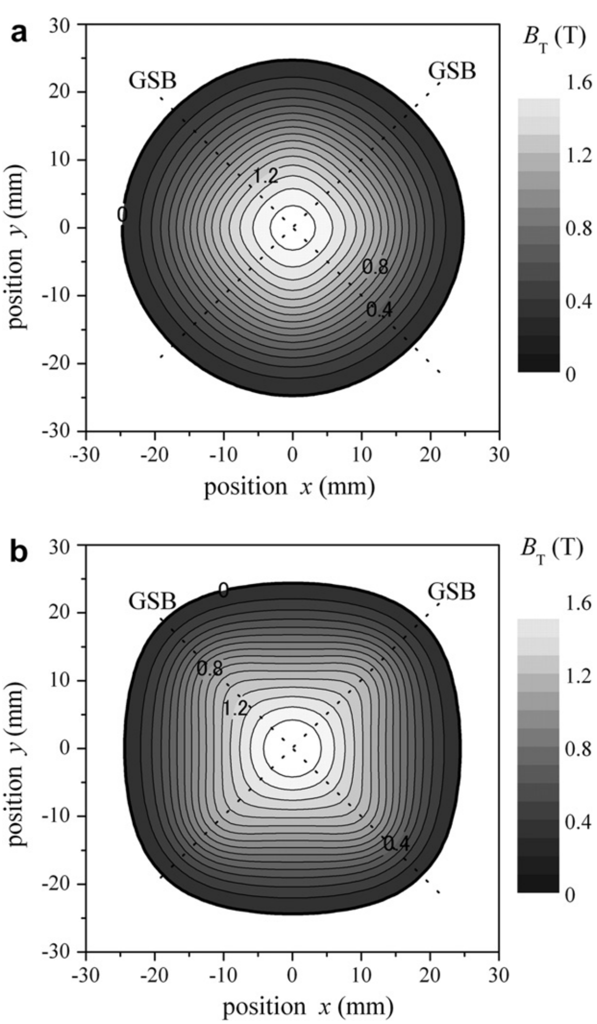

Fig. 4. Results of numerical calculation for magnetic field distributions in the horizontal plane 3.5 mm above the bulk surface for the applied pulsed-field of (a) $\mu_0 H = 3.83$ T and (b) $\mu_0 H = 4.64$ T, respectively.

4. Conclusions

We proposed a detailed simulation method which took into account the difference in the J_c characteristic between GSB and GSR parts. A Sm123 bulk superconductor was magnetized by the PFM as varying the magnitude of applied field and trapped field distribution was measured. The magnetic flux density of the GSR part was higher than that of GSB part for the pulsed-field of $\mu_0 H = 3.83$ T, but the relation was opposite for the case of $\mu_0 H = 4.64$ T. It was confirmed that the difference of J_c influenced the performance of trapped field. Next, the numerical analysis was performed based on the experiment data. The current density in GSB and GSR parts was separately evaluated and the magnetic field distribution was calculated. The numerical calculation results of trapped field distribution were corresponding to the experimental one, and therefore, it was confirmed to be able to analyze the current distribution in detail by the proposed method. We will carry out the magnetizing simulation on the IMRA, MPSC and MMPSC methods hereafter, and furthermore, there is a possibility that a better magnetizing method can be proposed.

Acknowledgment

This study was partially supported by the CREAT IWATE Project driven by the Japan Science and Technology Organization.

References

[1] M. Tomita, M. Murakami, Nature 421 (2003) 517.
[2] N. Saho, H. Isogami, T. Takagi, M. Morita, IEEE Trans. Appl. Supercond. 9 (1999) 398.
[3] Y. Yanagi, T. Matsuda, H. Hazama, K. Yokouchi, M. Yoshikawa, Y. Itoh, T. Oka, H. Ikuta, U. Mizutani, Physica C 426–431 (2005) 764.
[4] N. Koshizuka, K. Matsunaga, N. Yamachi, A. Kawaji, H. Hirabayashi, M. Murakami, M. Tomita, S. Une, S. Saito, M. Isono, H. Nasu, T. Maeda, F. Ishikawa, Physica C 412–414 (2004) 756.
[5] K. Yokoyama, T. Oka, H. Okada, Y. Fujine, A. Chiba, K. Noto, IEEE. Trans. Appl. Supercond. 13 (2002) 1592.

[6] U. Mizutani, T. Oka, Y. Itoh, Y. Yanagi, M. Yoshikawa, H. Ikuta, IEEE. Trans. Appl. Supercond. 6 (1998) 235.
[7] H. Ikuta, T. Hosokawa, H. Ishihara, M. Yoshikawa, Y. Yanagi, Y. Itoh, T. Oka, U. Mizutani, IEEE Trans. Appl. Supercond. 11 (2001) 3716.
[8] M. Sander, U. Shutter, R. Koch, M. Läser, Supercond. Sci. Technol. 13 (2000) 841.
[9] H. Fujishiro, T. Tateiwa, A. Fujiwara, T. Oka, H. Hayashi, Physica C 445–448 (2006) 334.
[10] H. Fujishiro, T. Oka, K. Yokoyama, K. Noto, Supercond. Sci. Technol. 16 (2003) 809.
[11] K. Yokoyama, M. Kaneyama, T. Oka, H. Fujishiro, K. Noto, Physica C 412–414 (2004) 688.